

Influence of the local heating position on the terahertz emission power from high-T_c superconducting Bi₂Sr₂CaCu₂O₈+ δ mesas

C. Watanabe, H. Minami, T. Kitamura, K. Asanuma, K. Nakade, T. Yasui, Y. Saiwai, Y. Shibano, T. Yamamoto, T. Kashiwagi, Richard A. Klemm, and K. Kadowaki

Citation: *Applied Physics Letters* **106**, 042603 (2015); doi: 10.1063/1.4906768

View online: <http://dx.doi.org/10.1063/1.4906768>

View Table of Contents: <http://scitation.aip.org/content/aip/journal/apl/106/4?ver=pdfcov>

Published by the AIP Publishing

Articles you may be interested in

Generation of electromagnetic waves from 0.3 to 1.6 terahertz with a high-T_c superconducting Bi₂Sr₂CaCu₂O₈+ δ intrinsic Josephson junction emitter
Appl. Phys. Lett. **106**, 092601 (2015); 10.1063/1.4914083

Broadly tunable, high-power terahertz radiation up to 73 K from a stand-alone Bi₂Sr₂CaCu₂O₈+ δ mesa
Appl. Phys. Lett. **105**, 202603 (2014); 10.1063/1.4902336

Bi₂Sr₂CaCu₂O₈ intrinsic Josephson junction stacks with improved cooling: Coherent emission above 1 THz
Appl. Phys. Lett. **105**, 122602 (2014); 10.1063/1.4896684

Powerful terahertz emission from Bi₂Sr₂CaCu₂O₈+ δ mesa arrays
Appl. Phys. Lett. **103**, 022602 (2013); 10.1063/1.4813536

Direct imaging of hot spots in Bi₂Sr₂CaCu₂O₈+ δ mesa terahertz sources
J. Appl. Phys. **113**, 133902 (2013); 10.1063/1.4795591

The advertisement features a photograph of the Model PS-100 cryogenic probe station, which is a complex piece of laboratory equipment with various mechanical components and a probe head. The background is a gradient of blue. The text 'Model PS-100' is in a large, bold, white font. Below it, 'Tabletop Cryogenic Probe Station' is in a smaller white font. The Lake Shore CRYOTRONICS logo is on the right, consisting of a stylized blue and white square icon followed by the company name in white. At the bottom right, the tagline 'An affordable solution for a wide range of research' is written in a white, italicized font.

Model PS-100
Tabletop Cryogenic
Probe Station

 **Lake Shore**
CRYOTRONICS

*An affordable solution for
a wide range of research*

Influence of the local heating position on the terahertz emission power from high- T_c superconducting $\text{Bi}_2\text{Sr}_2\text{CaCu}_2\text{O}_{8+\delta}$ mesas

C. Watanabe,¹ H. Minami,^{1,2} T. Kitamura,¹ K. Asanuma,¹ K. Nakade,¹ T. Yasui,¹ Y. Saiwai,¹ Y. Shibano,¹ T. Yamamoto,³ T. Kashiwagi,^{1,2} Richard A. Klemm,⁴ and K. Kadowaki^{1,2}

¹Graduate School of Pure and Applied Sciences, University of Tsukuba, 1-1-1 Tennodai, Tsukuba, Ibaraki 305-8573, Japan

²Division of Materials Science, Faculty of Pure and Applied Sciences, University of Tsukuba, 1-1-1 Tennodai, Tsukuba, Ibaraki 305-8573, Japan

³Wide Bandgap Materials Group, Optical and Electronic Materials Unit, Environment and Energy Materials Division, National Institute for Materials Science, 1-1 Namiki, Tsukuba, Ibaraki 305-0044, Japan

⁴Department of Physics, University of Central Florida, Orlando, Florida 32816-2385, USA

(Received 6 October 2014; accepted 26 December 2014; published online 29 January 2015)

Simultaneous measurements of spectroscopic terahertz emissions from and SiC photoluminescent local temperature $T(r)$ distributions of high transition temperature T_c superconducting $\text{Bi}_2\text{Sr}_2\text{CaCu}_2\text{O}_{8+\delta}$ rectangular mesa devices were made. A local region with $T(r) > T_c$ known as a hot spot can emerge with current bias changes. When the hot spot position was moved to a mesa end by locally heating the mesa surface with a laser beam, the intensity of the emission increased, but no changes to its frequency or line width were observed. These results suggest that higher power radiation is attainable by adjusting the hot spot position. © 2015 AIP Publishing LLC.

[<http://dx.doi.org/10.1063/1.4906768>]

The recent discovery of coherent THz emission from mesa structures of the high transition temperature T_c superconductor $\text{Bi}_2\text{Sr}_2\text{CaCu}_2\text{O}_{8+\delta}$ (Bi2212) has brought an enormous potential for THz sources characterized by coherent, continuous, and either monochromatic or tunable radiation.^{1–3} In particular, these superconducting THz emitters span the entire frequency range of 0.3–2.0 THz, filling the “THz gap” frequency range between 1 and 2 THz still lacking in good sources.⁴

The superconducting THz emitter consists of a stack of alternating superconducting double CuO_2 layers and insulating Bi_2O_2 layers forming intrinsic Josephson junctions (IJJs) along the c -axis direction. For emission from the stack of IJJs, the following two conditions have to be fulfilled: The ac-Josephson effect that transforms the applied dc-voltage V across the N IJJs to a high-frequency ac-current and photon emission at frequency $f = (2e/h)v$, where $v = V/N$, e is the elementary charge, and h is the Planck’s constant.⁵ Another condition to be satisfied is the electromagnetic cavity resonance condition that enhances a particular excitation mode of the superconducting plasma waves in the mesa. For a rectangular cavity, the excited mode is usually that of a half wavelength across the mesa width w , with $f = c_0/2nw$, where c_0 is the speed of light in vacuum and n is the refractive index of Bi2212.¹ Although this radiation has the considerable power P of several $10 \mu\text{W}$, it may not be sufficient for many applications.⁶ Since $P \propto N^2$, increasing N could, in principle, enhance P greatly.^{7–9} However, in practice, thicker mesas lead to considerably larger Joule heating, which can drive the local mesa temperature $T(r)$ above T_c in a region known as a “hot spot,”^{10–13} greatly limiting the emission P . Indeed, enormously inhomogeneous $T(r)$ distributions in a mesa were observed by low temperature scanning laser microscopy (LTSLM)^{14–16} and by photoluminescence (PL) techniques,^{17,18} and were predicted by numerical simulations.^{19,20} More recently, by directly measuring the mesa

$T(r)$ using the photoluminescence of attached SiC microcrystals during simultaneous spectroscopical investigations of the THz radiation from the Bi2212 devices, we also confirmed the formation of a hot spot in the higher current I bias region of the I - V characteristics (IVCs).^{21,22} Furthermore, small changes in the I bias were found to lead to sudden jumps in the hot-spot position plus strong changes in the emission intensity.²² These observations strongly suggest that the emission intensity from the mesa may be sensitive to the hot-spot position, and therefore may be enhanced by carefully controlling it. This behavior was also found in numerical simulations of local heating effects on Bi2212 mesas.^{23,24}

The mesas used for the present measurements were fabricated as described previously.^{21,22,25,26} The dimensions of Mesa L were measured by an atomic force microscope to be $400 \mu\text{m}$ in length, $79 \mu\text{m}$ in upper width, $89 \mu\text{m}$ in lower width, and $2.4 \mu\text{m}$ in thickness, including the thickness of the electrode pad (see Fig. 1(a)). Mesa L, highlighted by the solid red rectangle, was then uniformly embrocated by SiC fine powder in order to measure $T(r)$, as shown in Fig. 1(b).

A schematic view of the experimental setup is shown in Fig. 1(c), which represents the technique of controlling the hot-spot position with an external laser beam. We used both blue and red lasers, with respective wave lengths of 405 nm and 660 nm, each having a maximum power of about 80 mW, sufficient for this purpose. The laser was attached to an external manipulator, as shown in Fig. 1(c). The laser spot can be focused within the width of the mesa (about $80 \mu\text{m}$ in diameter). The sample was mounted on the Cu cold finger of the He-flow cryostat by silver paste. UV light with a central wave length of 375 nm emitted from a commercial UV-light emitting diode (UV-LED) was uniformly irradiated upon the mesa device. In order to measure the mesa $T(r)$, the blue component of the PL from the SiC microcrystals was recorded by a charge-coupled device (CCD) camera through

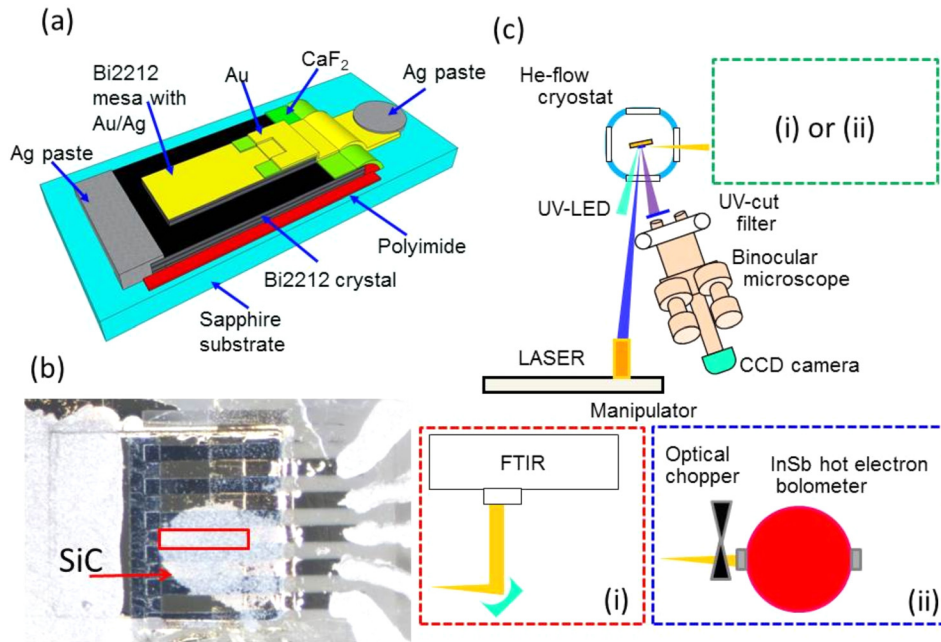


FIG. 1. (a) A stereographical drawing of the mesa device. (b) An optical photograph of the 5-mesa array structure. The solid red rectangle highlights Mesa L used in the present as well as in previous experiments.^{21,22} In order to measure $T(r)$ of the mesa, it was embrocated by SiC fine powder, shown as the light blue region indicated by the red arrow. (a) and (b) are taken from Figs. 1(a) and 1(b) in our previous letter.²² (c) A sketch of the optical setup for controlling the hot-spot position with either a blue or red laser beam, and for the simultaneous THz emission spectral measurements using either (i) an FTIR spectrometer or (ii) an InSb hot electron bolometer.

an objective lens at the angle of 20° tilted from the normal to the surface of the mesa device. Either the mesa's THz emission spectrum or its intensity could be, respectively, observed by a commercial FTIR spectrometer (FARIS-1, JASCO Corporation)²⁷ (indicated by (i)) or an InSb hot electron bolometer (indicated by (ii)) at the angle of 70° tilted from the normal, although it is not the ideal direction for the measurements.^{28,29}

The IVCs of the mesa at bath temperature $T_b = 25$ K under UV light radiation were first measured in the constant I mode without the laser beam. The results pictured in Fig. 2(a) show a typical IVC hysteresis curve and a drastic back-bending behavior due to significant self heating effects.^{19,20} The red circle indicates the point $I = 50.2$ mA of all subsequent PL and emission frequency spectral studies.

Then, to study the effect of the hot-spot position on the emission frequency, the blue laser was focused on four top device surface positions. In Fig. 2(b), optical images obtained from the CCD camera are shown in panels L1-L6. The red solid rectangles represent the position of Mesa L, and the many small blue dots arise from the PL of the fine SiC powder under UV light. Panels L1 and L6 were, respectively, obtained before and after the laser was applied to the device. The large bright white regions in panels L2-L5 arise from the laser beam and presumably from its reflections off the device edges. Since the PL intensity from the SiC powder decreases strongly with increasing temperature,^{21,22} the hot spot is observed in panels L1-L6 as the black regions in the optical images. Since the bright white spots due to the laser obscure the hot spot in panels L3 and L4, these regions and

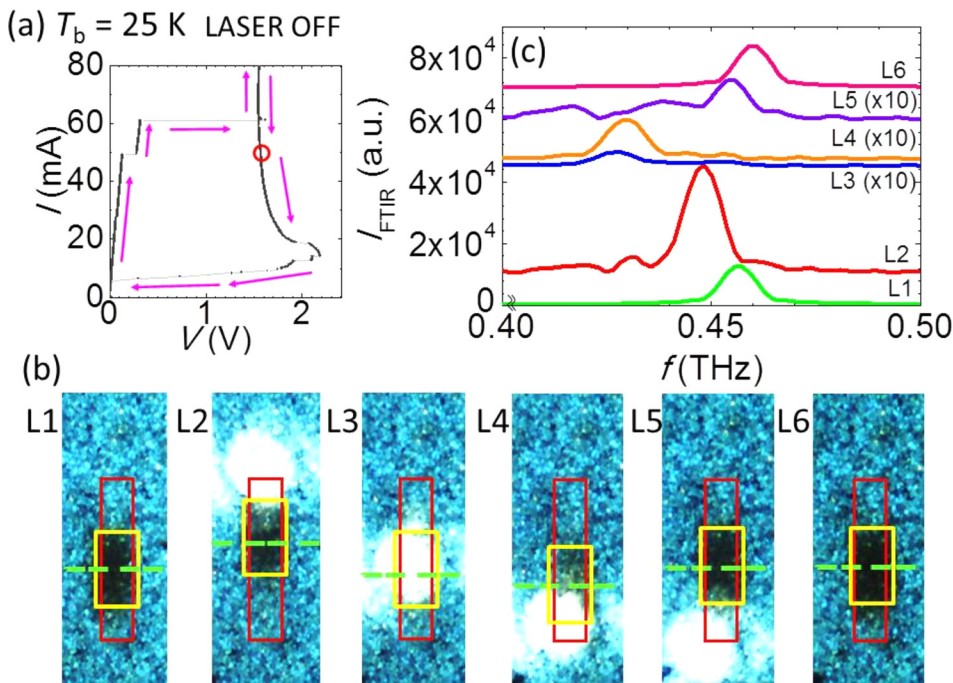


FIG. 2. (a) IVCs of Mesa L at $T_b = 25$ K under UV radiation without the laser. The red circle indicates the $I = 50.2$ mA point studied. (b) UV PL images L1 and L6 taken at $I = 50.2$ mA before and after the blue laser was turned on and off, respectively. UV PL images from L2 to L5 were taken at $I = 50.2$ mA with the blue laser beam applied over the white disk regions. The solid yellow rectangles and the horizontal dashed green lines indicate the hot-spot positions and their centers, respectively. The solid red rectangles highlight the fixed mesa position. (c) The emission spectra corresponding to L1 to L6 measured by the FTIR spectrometer.

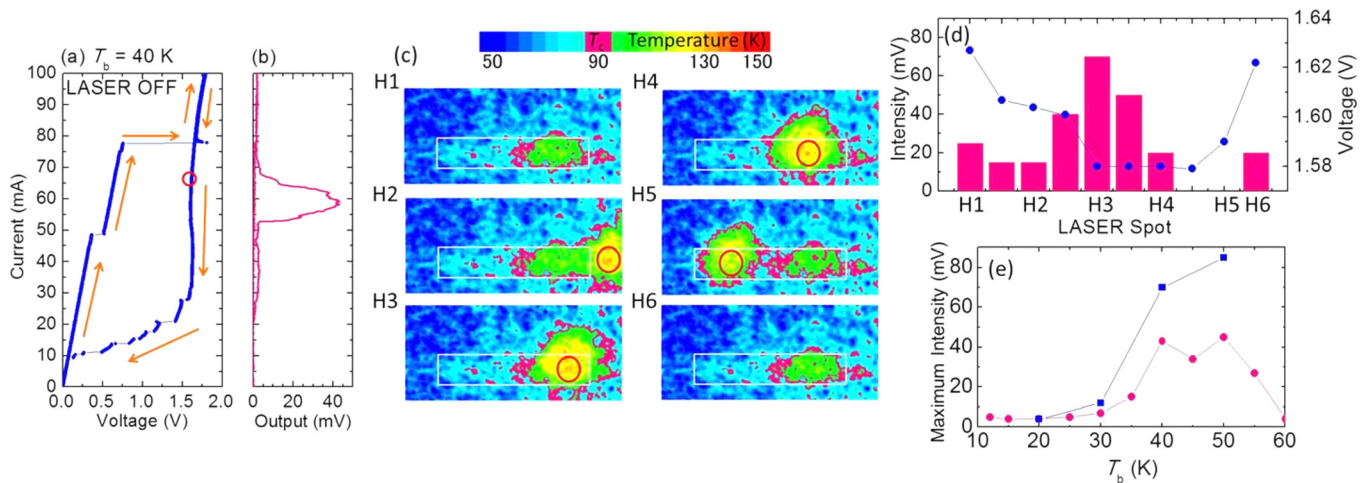


FIG. 3. (a) IVCs and (b) emission intensity of Mesa H versus I at $T_b = 40$ K. (c) Panels H1 to H6 indicate the color coded $T(r)$ of Mesa H at 40 K and $I = 65$ mA. The red circles indicate the center position of the focused laser spot. (d) Mesa H emission intensity (pink histogram, left scale) and V (blue filled dots, right scale). (e) T_b dependence of the maximum emission intensity when Mesa H was (blue dots) and was not (pink dots) irradiated by the red laser beam.

their centers are highlighted in panels L1-L6 by the solid yellow rectangles and the dashed horizontal green lines, respectively. When the laser beam is switched off, the hot spot can be observed in panel L6 to have returned to its original position shown in panel L1, just below the center of the mesa, as was observed previously.²¹ We note that this hot-spot position is far from the current feeding position at the upper end of Mesa L.

As soon as the laser beam is switched on and is focused on the top edge of Mesa L, as shown in panel L2 of Fig. 2(b), for example, the position of the hot spot changes sensitively. In panel L2 of Fig. 2(b), the hot-spot position has moved slightly up toward the laser beam. As the laser beam intensity is increased, the hot spot moves further up Mesa L, and its center eventually merges (not pictured) with the center of the laser spot. When the position of the laser beam is then shifted down the length of the mesa, the hot spot moves down with it, and is completely obscured by the laser spot, as shown in panel L3. Once this occurs, the hot spot cannot be separated from the laser beam until the laser nearly reaches the bottom edge (L4) of Mesa L. When the laser is centered just below the bottom edge of Mesa L, the hot spot moves up the mesa (L5). The hot spot returns to its original position after the laser beam is turned off (L6). Hence, the hot-spot position is controllable with the laser.

The remarkable feature observed here is that the THz radiation intensity varies strongly depending on the hot-spot position. This is seen in the spectral intensity data shown in Fig. 2(c), for which panels L1-L6 have a one-to-one correspondence with panels L1-L6 in Fig. 2(b). The THz emission intensity is much larger in panel L2 than in all the other panels of Fig. 2(c). Although it is not clear why the emission intensity is the strongest when the hot-spot position is nearest to the top of Mesa L as pictured in panel L2 of Fig. 2(b), it seems that the area of the superconducting region(s) or the position of the hot spot influences the emission intensity. In panel L3 of Fig. 2(b), the hot spot separates into two small superconducting regions, and the intensity shown in panel L3 of Fig. 2(c) is the weakest. However, there is an asymmetry in the overall behavior, as the superconducting regions in

panels L2 and L4 of Fig. 2(b) appear to have nearly equal areas, but the emission intensities are not the same in panels L2 and L4 of Fig. 2(c). This asymmetry is difficult to explain, although we note that in panel L2, the hot spot and the laser beam are near to the current feed position. It was also suggested previously that the strongest THz radiation was observed when the hot spot could not be observed at high T_b values, and the mesa had the greatest superconducting area.⁶ Note that the line width of the emission remains below our experimental resolution for all hot-spot positions, and the frequency of the emission only decreases by a few percent due to the hot-spot position. Since the quality Q factor of the TM₁₀ cavity mode resonance is rather low,² the emission f appears to satisfy the cavity resonance condition (420–480 GHz).

In order to better understand the mechanism of the increase of the intensity by controlling the hot-spot position, Mesa H was fabricated and $T(r)$ was measured in detail. Mesa H (not shown here) is $80\ \mu\text{m}$ in width, $400\ \mu\text{m}$ in length, and $2\ \mu\text{m}$ in height. The same experimental setup, as shown in Fig. 1(c), was used for the experiments. Since the photoluminescence of SiC powder has the strongest temperature T dependence for blue light,²¹ in the former measurements, both the SiC photoluminescence and the blue laser beam were detected by the blue CCD pixels. Therefore, it was not possible to accurately measure the local $T(r)$, especially in panel L3 of Fig. 2(b). This enabled us to track the position of the laser beam, but interfered with our $T(r)$ measurements. In order to better detect the $T(r)$ with the most sensitive blue CCD pixels, we used a red laser beam in our studies of Mesa H, and again used the blue CCD pixels to measure $T(r)$. The above experiments shown for Mesa L were also performed on Mesa H at various T values at various IVC points. As a result, although the position of the red laser beam was not directly detected, the red laser's considerable effects on the position of the hot spot and on the THz radiation were observed using Mesa H.

Before red laser irradiation, a typical example of the IVCs of Mesa H at $T_b = 40$ K is shown in Fig. 3(a), and the strong THz radiation observed is shown in Fig. 3(b).

In Fig. 3(c), we show the $T(r)$ obtained from Mesa H at $T_b = 40$ K and $I = 65$ mA, which is injected from the right hand side of the mesa. The white solid rectangles and the red solid circles, respectively, highlight the position of Mesa H and the central position of the red laser beam. Before this laser was turned on, the hot spot appears near to the I injection point at the right hand side of Mesa H, as seen in panel H1 of Fig. 3(c). This sometimes appears for mesas with larger contact resistances, because the I injection generates considerable extra heat that may attract the hot spot to the contact region.

As seen in panel H2 of Fig. 3(c), when the red laser beam is focused on the right edge of the mesa, more than half of the right hand side of the mesa was heated above T_c due to the additional heating of the laser beam. Then, the red laser beam was scanned from right to left on the mesa surface (H2-H5) and heats up the mesa near its point of impact, but the hot spot center mostly does not follow the laser beam. Figure 3(d) shows the emission intensity (the pink histogram) of the THz wave observed by the InSb hot electron bolometer and the applied V (the blue dots). It is surprising that the emission intensity in Fig. 3(d) corresponding to panel H3 of Fig. 3(c) is approximately three times as large as that corresponding to panel H1, before the red laser beam was turned on. However, the emission intensity suddenly decreases when the laser beam spot is moved only slightly from its position in panel H3 to its position in panel H4, and the area of the superconducting region of Mesa H deduced from panel H4 becomes somewhat smaller than that deduced from panel H3, but the V values corresponding to panels H3 and H4 are almost the same, as shown in Fig. 3(d). Eventually, the emission intensity drops almost to zero at laser spot position H5, as shown in Fig. 3(d), when the mesa was heated at the left side of the mesa as shown in panel H5 of Fig. 3(c), since $T(r) > T_c$ for nearly the entire mesa. Finally, the laser beam was turned off, and the $T(r)$ pictured in panel H6 of Fig. 3(c) and the corresponding emission intensity of laser spot H6 in Fig. 3(d) return to their original function shown in panel H1 of Fig. 3(c) and intensity value at spot point H1 in Fig. 3(d). These results are consistent with those described above for Mesa L, as shown in Figs. 2(b) and 2(c). We note, however, that the enhancement of the emission intensity indicated at laser spot H3 in Fig. 3(d) corresponding to the application of the laser beam as in panel H3 of Fig. 3(c) could not be observed when $I = 59$ mA, at which the overall emission intensity was the maximum (45 mV) in the absence of the laser, as shown in Fig. 3(b).

The reproducibility of the enhancement phenomenon by the laser beam control as well as the previous measurements were confirmed at $I = 65$ mA and $T_b = 40$ K. Moreover, this phenomenon was observed at the wide T_b region between 30 and 50 K, as shown in Fig. 3(e), until about 50 K above which the hot spot was no longer observed. In Fig. 3(e), the pink dots represent the maximum emission intensity when the mesa was not heated by the red laser beam, while the blue solid squares indicate the maximum emission intensity when the mesa was heated by the red laser beam. It is evident that the THz emission intensity of 90 mV as measured by the InSb hot electron bolometer at 50 K with the laser beam is twice as high as that (45 mV) without the laser

beam, when the laser beam is adjusted so as to have the maximum power emission. It is noted that such an enhancement of the emission intensity could not be achieved if the mesa were not heated locally by the focused laser beam.

In conclusion, we could enhance the THz emission power by manipulating the position of the hot spot by heating the mesa locally using a focused laser beam. The experimental results clearly show that the THz emission intensity can be enhanced by at least a factor of two by adjusting the hot-spot position by local laser beam heating. Although the mechanism of the enhancement of the THz emission is still not well understood, it is evident that the area and location of the normal part of the mesa play very important roles for the high power emission, consistent with previous work on stand-alone mesas.^{6,30–32}

The authors express sincere thanks to Dr. M. Tsujimoto, Mr. S. Sekimoto, and to other colleagues, for stimulating discussions. They also thank Professor Dr. R. Kleiner, Dr. H. B. Wang, Dr. W.-K. Kwok, Dr. U. Welp, and Professor R. Yoshizaki for fruitful discussions. This work was supported in part by the Grant-in-Aid for challenging Exploratory Research from the Ministry of Education, Culture, Sports, Science and Technology. C. Watanabe was supported by the JSPS Research Fellowship for young scientists.

- ¹L. Ozyuzer, A. E. Koshelev, C. Kurter, N. Gopalsami, Q. Li, M. Tachiki, K. Kadowaki, T. Yamamoto, H. Minami, H. Yamaguchi, T. Tachiki, K. E. Gray, W.-K. Kwok, and U. Welp, *Science* **318**, 1291 (2007).
- ²U. Welp, K. Kadowaki, and R. Kleiner, *Nat. Photonics* **7**, 702 (2013).
- ³K. Kadowaki, H. Yamaguchi, K. Kawamata, T. Yamamoto, H. Minami, I. Kakeya, U. Welp, L. Ozyuzer, A. Koshelev, C. Kurter, K. E. Gray, and W.-K. Kwok, *Physica C* **468**, 634 (2008).
- ⁴M. Tonouchi, *Nat. Photonics* **1**, 97 (2007).
- ⁵B. D. Josephson, *Phys. Lett.* **1**, 251 (1962).
- ⁶S. Sekimoto, C. Watanabe, H. Minami, T. Yamamoto, T. Kashiwagi, R. A. Klemm, and K. Kadowaki, *Appl. Phys. Lett.* **103**, 182601 (2013).
- ⁷C. Varnazis, R. D. Sandell, A. K. Jain, and J. E. Lukens, *Appl. Phys. Lett.* **33**, 357 (1978).
- ⁸D. R. Tilley, *Phys. Lett. A* **33**, 205 (1970).
- ⁹F. Song, F. Müller, R. Behr, and A. M. Klushin, *Appl. Phys. Lett.* **95**, 172501 (2009).
- ¹⁰A. V. Gurevich and R. G. Mints, *Rev. Mod. Phys.* **59**, 941 (1987).
- ¹¹W. J. Skocpol, M. R. Beasley, and M. Tinkham, *J. Appl. Phys.* **45**, 4054 (1974).
- ¹²F. Turkoglu, H. Koseoglu, Y. Demirhan, L. Ozyuzer, S. Preu, S. Malzer, Y. Simsek, P. Müller, T. Yamamoto, and K. Kadowaki, *Supercond. Sci. Technol.* **25**, 125004 (2012).
- ¹³C. Kurter, L. Ozyuzer, T. Proslir, J. F. Zasadzinski, D. G. Hinks, and K. E. Gray, *Phys. Rev. B* **81**, 224518 (2010).
- ¹⁴H. B. Wang, S. Guéron, J. Yuan, A. Iishi, S. Arisawa, T. Hatano, T. Yamashita, D. Koelle, and R. Kleiner, *Phys. Rev. Lett.* **102**, 017006 (2009).
- ¹⁵H. B. Wang, S. Guéron, B. Gross, J. Yuan, Z. G. Jiang, Y. Y. Zhong, M. Grünzweig, A. Iishi, P. H. Wu, T. Hatano, D. Koelle, and R. Kleiner, *Phys. Rev. Lett.* **105**, 057002 (2010).
- ¹⁶S. Guéron, M. Grünzweig, B. Gross, J. Yuan, Z. G. Jiang, Y. Y. Zhong, M. Y. Li, A. Iishi, P. H. Wu, T. Hatano, R. G. Mints, E. Goldobin, D. Koelle, H. B. Wang, and R. Kleiner, *Phys. Rev. B* **82**, 214506 (2010).
- ¹⁷S. Niratisairak, Ø. Haugen, T. H. Johansen, and T. Ishibashi, *Physica C* **468**, 442–446 (2008).
- ¹⁸T. M. Benseman, A. E. Koshelev, W.-K. Kwok, U. Welp, V. K. Vlasko-Vlasov, K. Kadowaki, H. Minami, and C. Watanabe, *J. Appl. Phys.* **113**, 133902 (2013).
- ¹⁹B. Gross, S. Guéron, J. Yuan, M. Y. Li, J. Li, A. Ishii, R. G. Mints, T. Hatano, P. H. Wu, D. Koelle, H. B. Wang, and R. Kleiner, *Phys. Rev. B* **86**, 094524 (2012).
- ²⁰A. Yurgens, *Phys. Rev. B* **83**, 184501 (2011).

- ²¹H. Minami, C. Watanabe, K. Sato, S. Sekimoto, T. Yamamoto, T. Kashiwagi, R. A. Klemm, and K. Kadowaki, *Phys. Rev. B* **89**, 054503 (2014).
- ²²C. Watanabe, H. Minami, T. Yamamoto, T. Kashiwagi, R. A. Klemm, and K. Kadowaki, *J. Phys.: Condens. Matter* **26**, 172201 (2014).
- ²³H. Asai, M. Tachiki, and K. Kadowaki, *Appl. Phys. Lett.* **101**, 112602 (2012).
- ²⁴H. Asai and S. Kawabata, *Appl. Phys. Lett.* **104**, 112601 (2014).
- ²⁵T. Mochiku, K. Hirata, and K. Kadowaki, *Physica C* **282–287**, 475–476 (1997).
- ²⁶H. Minami, M. Tsujimoto, T. Kashiwagi, T. Yamamoto, and K. Kadowaki, *IEICE Trans. E* **95-C**, 347 (2012).
- ²⁷Contact address: JASCO Corporation, 2967-5, Ishikawamachi Hachiojishi, Tokyo, Japan, TEL.: +81-42-646-4111. FAX: +81-42-646-4120. The instrumental spectral resolution is 7.5 cm^{-1} .
- ²⁸R. A. Klemm, E. R. LaBerge, D. R. Morley, T. Kashiwagi, M. Tsujimoto, and K. Kadowaki, *J. Phys.: Condens. Matter* **23**, 025701 (2011).
- ²⁹K. Kadowaki, M. Tsujimoto, K. Yamaki, T. Yamamoto, T. Kashiwagi, H. Minami, M. Tachiki, and R. A. Klemm, *J. Phys. Soc. Jpn.* **79**, 023703 (2010).
- ³⁰M. Tsujimoto, T. Yamamoto, K. Delfanazari, R. Nakayama, T. Kitamura, M. Sawamura, T. Kashiwagi, H. Minami, M. Tachiki, K. Kadowaki, and R. A. Klemm, *Phys. Rev. Lett.* **108**, 107006 (2012).
- ³¹M. Ji, J. Yuan, B. Gross, F. Rudau, D. Y. An, M. Y. Li, X. J. Zhou, Y. Huang, H. C. Sun, Q. Zhu, J. Li, N. Kinev, T. Hatano, V. P. Koshelets, D. Koelle, R. Kleiner, W. W. Xu, B. B. Jin, H. B. Wang, and P. H. Wu, *Appl. Phys. Lett.* **105**, 122602 (2014).
- ³²T. Kitamura, T. Kashiwagi, T. Yamamoto, M. Tsujimoto, C. Watanabe, K. Ishida, S. Sekimoto, K. Asanuma, T. Yasui, K. Nakade, Y. Shibano, Y. Saiwai, H. Minami, R. A. Klemm, and K. Kadowaki, *Appl. Phys. Lett.* **105**, 202603 (2014).